

MET O 19 BRANCH MEMORANDUM No...³⁴.....



The Retrieval of Meteorological Data from VTPR clear radiances; Part 1 - Retrieval of Surface and atmospheric radiation.

124052

by

B R May & F Rawlins.

Met O 19
(High Atmosphere Branch)
Meteorological Office
London Road
BRACKNELL
Berks RG12 2SZ

December 1976.

Note: This paper has not been published. Permission to quote from it should be obtained from the Assistant Director of the above Meteorological Office Branch.

FH3B

The Retrieval of Meteorological Data from VTPR Clear Radiances:Part 1 - Retrieval of Surface and Atmospheric Radiation

by B R May and F Rawlins

Abstract:-

The Vertical Temperature Profile Radiometer (VTPR) clear radiances usually contain components of radiation from both the surface and atmosphere. In this paper a description is given of the radiometric characteristics of the VTPR which leads to a technique for retrieving separately the two components based on results calculated from a sample of model atmospheres. The method is applicable to radiances observed over any surface and results for the dependent sample of atmospheres demonstrate its effectiveness. The sources and characteristics of VTPR clear radiances are discussed.

1. Introduction

This paper is one of a series concerned with the retrieval of meteorological data from cloud-free radiances measured by the Vertical Temperature Profile Radiometer (VTPR).

The VTPR is a scanning radiometer, currently flown on the NOAA operational space-craft, which measures the out-going atmospheric radiation at eight wavelengths in the infra-red spectral region. Six of these wavelengths are situated in the 15 micron CO_2 molecular band (channels 1 to 6 inclusive) and the radiances in these channels are used to deduce the atmospheric temperature. A further wavelength (channel 7) is in an H_2O molecular band whose radiance provides information about water-vapour in the atmosphere. The remaining wavelength (channel 8) is situated in a window region. The instantaneous field of view of the VTPR at the nadir is 60×60 km elongating to 60×90 km at the ends of the scan.

Many methods of retrieving meteorological data (thickness, temperature, humidity) from cloud-free atmospheric radiances such as those measured by the VTPR have been described in the literature. These include the Minimum Information and the Regression methods, both of which have been used by the U.S. National Environmental Satellite Service (NESS) to retrieve the SIRS soundings from VTPR clear radiances. Others include Chahine's, the Maximum Probability and the Eigenvector methods. These methods are described in reference 1.

Now clear VTPR radiances are not solely the atmospheric radiances because they may also contain a proportion of surface radiation. In the retrieval methods mentioned previously (as described in the literature) no specific attempt is made to isolate the atmospheric radiances before attempting to use them to retrieve meteorological data. The authors of this paper feel that there may be some benefit in doing this because the spatial patterns of atmospheric radiance could then be used as a visual guide in forecasting as well as being converted into thicknesses or humidities for objective analyses.

In section 2 of this paper we describe the radiometric characteristics of the VTPR as a preliminary to developing in section 3 the method of retrieving the Black-body radiation emitted by the surface and atmosphere (and hence their temperatures) from clear radiances. It is assumed that the atmospheric radiation is emitted by atmospheres similar to members of a sample of latitude and monthly means. Results indicating the effectiveness of the method are given for the dependent sample in section 4. The method described here can be used over both land and sea and in section 5 we discuss the consequences of this on techniques which can be used to obtain clear radiances.

In further papers we propose to present a) relationships between the atmospheric radiances and the water-vapour content and selected atmospheric thicknesses, with results from the dependent sample, and b) comparisons of retrieved meteorological data with conventional measurements.

2. Radiometric characteristics of the VTPR channels

In order to derive the equations to be used to retrieve the surface and atmospheric contributions to the clear radiance it is necessary to introduce the radiative transfer equation as applied to the VTPR channels.

The out-going clear radiance R_i observed in VTPR channel i can be expressed as

$$R_i = B(T_s, \bar{\nu}_i) \epsilon \tau_i^s + \int_{\tau_i^p=1.0}^{\tau_i^p=\tau_i^s} B(T^p, \bar{\nu}_i) \frac{d\tau_i^p}{df(p)} \cdot df(p) \quad (1)$$

where the first and second terms on the R.H.S of equation 1 are contributions from the surface and atmosphere respectively. In this equation $B(T, \bar{\nu})$ is the Black-body radiation given by the Planck function for temperature T and wave-number $\bar{\nu}$, T_s and T^p are the temperatures of the surface and the atmospheric pressure level p respectively, $\bar{\nu}_i$ is the wave number of the i th channel and ϵ is the emissivity of the surface. τ_i^p is the atmospheric transmission from the pressure level p to the top of the atmosphere and $f(p)$ is a function of pressure;

$d\bar{x}_i^p/d\bar{f}(p)$ is the weighting function of the i th channel which governs the contribution of radiation emitted by each atmospheric layer to the emerging radiation.

Throughout this paper the Black-body radiation, and hence radiances, are expressed in radiance units (RU) of one $mW.m^{-2}.sr^{-1}(cm^{-1})^{-1}$. Table 1 gives the Black-body radiation as a function of temperature for $\bar{\nu} = 700 \text{ cm}^{-1}$, along with the change in radiation per degree change in temperature. The significance of the choice of $\bar{\nu} = 700 \text{ cm}^{-1}$ is explained in section 3.

Table 1 - Black-body radiation at $\bar{\nu} = 700 \text{ cm}^{-1}$

| Temperature T (K) | B(T) (RU) | dB(T)/dT (RU.K ⁻¹) |
|----------------------|--------------|-----------------------------------|
| 220 | 42.4 | 0.9 |
| 230 | 51.9 | 1.0 |
| 240 | 62.4 | 1.1 |
| 250 | 74.0 | 1.2 |
| 260 | 86.7 | 1.3 |
| 270 | 100.4 | 1.4 |
| 280 | 115.1 | 1.5 |
| 290 | 130.7 | 1.6 |
| 300 | 147.4 | 1.7 |

Table 2 gives the approximate wave number and wavelength of the eight VTPR channels (the $\bar{\nu}_i$ for each individual VTPR are slightly different).

Table 2. $\overline{\nu}_i$ for the VTPR radiometric channels

| Channel number | $\overline{\nu}_i$ (cm^{-1}) | λ (microns) |
|----------------|---|---------------------|
| 1 | 669 | 15.0 |
| 2 | 678 | 14.8 |
| 3 | 695 | 14.4 |
| 4 | 708 | 14.1 |
| 5 | 725 | 13.8 |
| 6 | 747 | 13.4 |
| 7 | 535 | 18.7 |
| 8 | 833 | 12.0 |

Channel 1 is situated close the centre of the 15 micron CO_2 molecular band at the position of maximum absorption which results in a transmission and weighting function at the lowest atmospheric pressure (greatest height). The remaining CO_2 channels, numbers 2 to 6, lie to the short wave side of the 15 micron band at positions of successively decreasing absorption giving rise to a sequence of weighting functions at increasing atmospheric pressure. In the absence of water-vapour the transmission and weighting functions of channels 1 to 6 would be fixed with respect to the atmospheric pressure scale (apart from a slight variation with temperature) due to the constant mixing ratio of CO_2 to air, although τ_i^s would vary slightly due to changes in surface atmospheric pressure. However the short-wave wing of the water-vapour molecular band extending down to about 9 microns causes noticeable additional absorption in the CO_2 channels, decreasing the τ_i^p and modifying the shape of the weighting functions. The effect is most important for channels 5 and 6 whose weighting functions peak close to the surface where the greatest concentration of water-vapour is to be found. Channel 7 is situated in the strong water-vapour absorption band (in a spectral region free from CO_2 absorption) and, as a consequence its transmission and weighting functions are sensitively dependent upon the amount and distribution of water vapour in the atmosphere. As a rule, the peak of the

channel 7 weighting function is situated at the level above which there is about 0.8 gm of water vapour per cm^2 . Channel 8 is the "window" channel in that it is situated in a spectral region in which atmospheric absorption has a local minimum; absorption by CO_2 is negligible but absorption by water-vapour is not, resulting in a modification of the surface radiation reaching the top of the atmosphere in moist conditions.

The transmission functions τ_i^p for a low-latitude temperature profile in the dry and saturated conditions are shown in figure 1 and the weighting functions $d\tau_i^p/d(p^{2/3})$ in figure 2.

1. These transmission and weighting functions are for the radiometer observing at the nadir; because of the increased air mass along an inclined path the τ_i^s decrease when the radiometer scans to the side of the sub-satellite track. The change in τ_i^s in going from the vertical to 30° inclination ~~to~~ the vertical is about 5%.

From this brief description of the radiometric characteristics of the VTPR channels it can be seen for channel 4 to 8 the clear radiance consists of a surface contribution varying with T_s and ϵ and an atmospheric contribution varying with atmospheric temperature; the relative magnitude of these contributions also varies with the amount and distribution of water vapour.

We now proceed to consider how these contributions can be separated.

3. The Method of separating atmospheric and surface radiance components.

The smoothing effect of the considerable depth of the weighting functions in figure 2 results in atmospheric radiances which are averaged products from the atmospheric Planck profile. Since these radiances contain little information about small-scale vertical variations of T^p (or moisture) they are best regarded as being related to mean temperatures of appropriate atmospheric slabs from which thicknesses or total water-vapour contents can be deduced.

For the i th VTPR channel the atmosphere is regarded as being isothermal with a temperature T_i , overlying a surface of temperature T_s and emissivity ϵ . The T_i , which are effectively the mean temperatures in regions defined by the weighting functions, are different for each channel but the T_s and ϵ are the same.

Equation 1 can now be simplified to

$$R_i = B(T_s, \bar{\nu}_i) \epsilon \tau_i^s + B(T_i, \bar{\nu}_i) (1 - \tau_i^s) \quad (2)$$

Now the R_i are measured at the different wave numbers $\bar{\nu}_i = 1, 8$; in order to remove the frequency dependence of the Planck function, the R_i are normalised to a reference wave number $\bar{\nu}_{ref}$ (chosen to be 700 cm^{-1} in practice) by converting them to an intermediate temperature using $\bar{\nu} = \bar{\nu}_i$ and then back to radiances using $\bar{\nu} = \bar{\nu}_{ref}$. This normalisation procedure is not exact but produce only small errors because of the small range in the $\bar{\nu}_i$.

The dependence of radiance on $\bar{\nu}_i$ and the superscript s can now be omitted (but the subscript s is retained to denote surface temperature), giving

$$R_i = B(T_s) \epsilon \tau_i + B(T_i) (1 - \tau_i) \quad (3)$$

Because channel 8 is the window channel, R_8 contains the greatest proportion of information about the surface radiation so by combining the expressions for R_i and R_8 to eliminate $B(T_s) \epsilon$ we obtain an expression for $B(T_i)$

$$B(T_i) = \frac{[R_i \tau_8 - R_8 \tau_i]}{[(\tau_8 - \tau_i) + (1 - F_i) \tau_i (1 - \tau_8)]} \quad (4)$$

where

$$F_i = B(T_8) / B(T_i) \quad (5)$$

The second term in the denominator of equation 4, which allows for the difference in the temperatures of the atmospheric regions sensed by the weighting functions of the i th and the 8th channel, is usually very small compared with the

first term. For channels 1, 2 and 3, the τ_i are all zero and equation 4 reduces

to the trivial form $B(T_i) = R_i$

In practice the τ_i and F_i for use in equation 4 are determined using the iterative procedure described in section 4. The resulting $B(T_i)$ can then be used to calculate

$B(T_s) \epsilon$ from the channel 8 radiance using the equation

$$B(T_s) \epsilon = \frac{[R_8 - B(T_8)(1 - \tau_8)]}{\tau_8} \quad (6)$$

where $B(T_8) = B(T_i) \cdot F_i$ from any channel.

Although the atmospheric and surface contributions to the out-going radiation observed above the atmosphere are strictly $B(T_i)(1 - \tau_i)$ and $B(T_s) \epsilon \tau_i$ we concentrate our attention on $B(T_i)$ and $B(T_s) \epsilon$ for the following reasons:-

- a. The expression for $B(T_i)$ has a useful degree of self-compensation against small changes in the τ_i and τ_8 because these transmissions occupy the same relative positions in the numerator and denominator of equation 4; this also applies to τ_8 in the expression for $B(T_s) \epsilon$ (equation 6). $B(T_i)(1 - \tau_i)$ and $B(T_s) \epsilon \tau_i$ do not have this property.
- b. Atmospheric thicknesses, humidities and surface temperatures are derived from the $B(T_i)$ and $B(T_s) \epsilon$ (to be discussed in a future paper), not $B(T_i)(1 - \tau_i)$ and $B(T_s) \epsilon \tau_i$

As a consequence of a) above, we do not differentiate between clear radiances measured at angles up to 30° inclination to the nadir, which varies the τ_i

For the calculation of the $B(T_i)$ and $B(T_s) \epsilon$ using equations 4 and 6, estimates are required of the τ_i and the F_i . In the absence of water vapour in the atmosphere the τ_i could be regarded as near-constant (with some slight dependence upon atmospheric temperature) but figures 1 and 3 show that they are sensitively dependent upon the water-vapour content. The channel 7 radiance is the most sensitive

indicator of water-vapour amount, which determines the height of the weighting function, but the radiance also depends upon the atmospheric temperature at that height. The water-vapour content and hence the τ_i are therefore not expected to be functions of $B(T_7)$ alone but functions of $B(T_7)$ and the remaining $B(T_i)$, $i = 1, 6$, the latter allowing for the temperature dependence. From a consideration of the relative positions of the VTPR weighting functions in the atmosphere it appears that the radiance in channel 6 most closely monitors the atmospheric temperature in the region of the weighting function of channel 7 in near-average humidity conditions, so we seek to express the τ_i in terms of $B(T_6)$ and $B(T_7)$.

In order to establish the nature of the dependence of the τ_i on $B(T_6)$ and $B(T_7)$ calculations of vertical transmissions and radiances from a sample of temperature and humidity profiles were carried out. The τ_i were calculated using a polynomial transmissions model for VTPR instrument 2 on NOAA4 spacecraft which was supplied by M Weinreb of NESS. In order to provide a range of temperature conditions the set of monthly mean atmospheric temperature profiles for latitude bands centred on 15° , 30° , 45° and 60°N were selected; these were used with the accompanying monthly mean humidity profiles, and also saturated and dry to provide results for extreme conditions of humidity (144 model atmospheres in all). The R_i were calculated from equation 1 using monthly mean sea-surface temperatures for the same latitude bands as the atmosphere and $\epsilon = 0.99$ in order to provide realistic surface radiance contributions. These R_i were normalised to $\bar{\nu} = 700 \text{ cm}^{-1}$ as described previously. The $B(T_i)$ were then derived using equation 3 where $B(T_5)$ was calculated directly from T_s using $\bar{\nu} = 700 \text{ cm}^{-1}$.

It was found by experiment that the τ_i were closely related to $B(T_6)$ and $B(T_7)$ by the functions

$$\tau_i = f(B(T_7) - a_i B(T_6)) \quad (7)$$

which are shown in figure 3, where the a_i have the values in table 3.

Table 3

Values of a_i

| Channel number | a_i |
|----------------|-------|
| 4 | 1.93 |
| 5 | 1.75 |
| 6 | 1.64 |
| 7 | 1.54 |
| 8 | 1.46 |

In order to establish the limiting values of f_7 and f_8 for dry atmospheres (for which $\tau_7 = \tau_8 = 1.0$ and hence $B(T_7)$ and $B(T_8)$ are undefined) it was assumed that T_7 and T_8 both tend to the surface atmospheric temperature as the weighting functions of these channels diminish.

The solutions of equations 4 and 6 also require values of the F_i and it was found that, like the τ_i they could also be represented by the functions

$$F_i = f(B(T_7) - b_i B(T_6)) \quad (8)$$

which are shown in figure 4, where the b_i have the values in table 4.

Table 4

Values of b_i

| Channel number | b_i |
|----------------|-------|
| 5 | 1.02 |
| 6 | 1.21 |
| 7 | 1.22 |

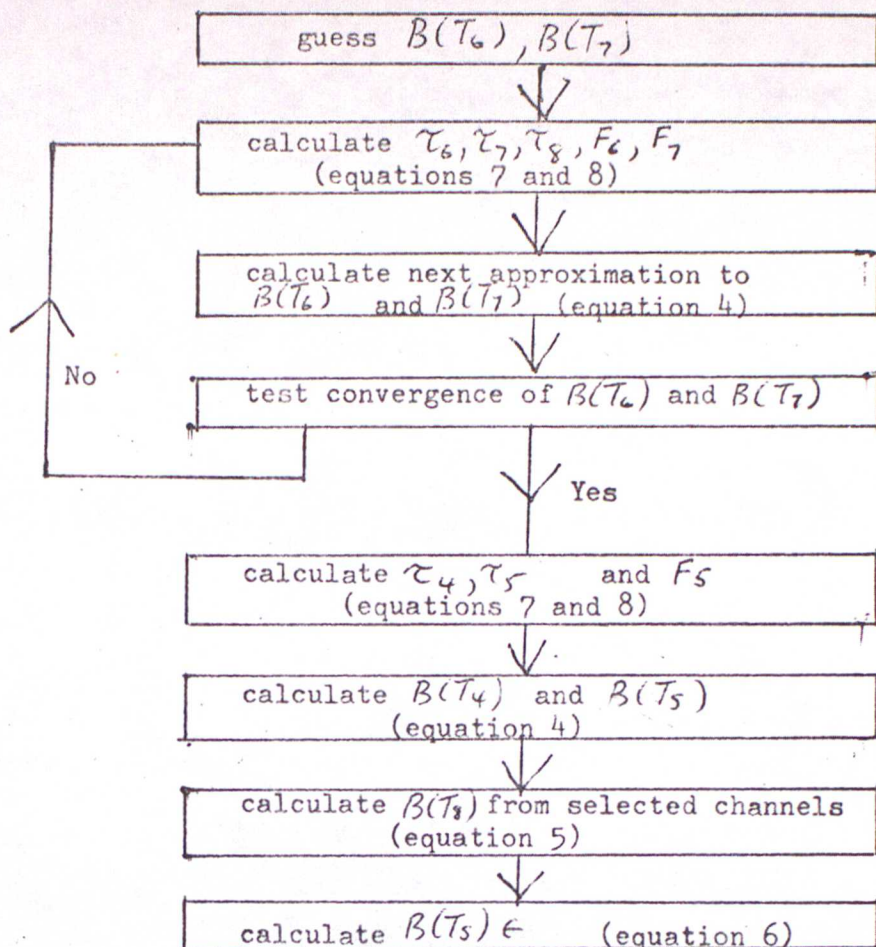
For channel 4 it was found to be adequate to use the fixed value $F_4 = 2.13$ while for channels 1, 2 and 3 the F_i are irrelevant since τ_1 , τ_2 and τ_3 are always zero.

Equations 4 to 8, along with the functions in figures 3 and 4 and the constants in tables 3 and 4, can be used to retrieve the $B(T_c)$ and $B(T_s)$ strictly only from the R_i measured by VTPR instrument 2 on NOAA4 spacecraft. However it is believed that the form of the equations and the general shape of the functions apply to all VTPR's and that only small adjustments to the functions and constants are needed for different instruments. It must also be stressed that the method is model-dependent. The $B(T_c)$ are retrieved from the R_i assuming that the radiances are emitted by atmospheres similar to those of the sample. However we hope to reduce the model dependence by concentrating attention on the retrieval of suitably averaged quantities such as the T_i or total amounts of water vapour which are more obviously related to the radiances produced by broad weighting functions.

The method follows naturally from the Radiative Transfer Equation expressed in its simplest form as applied to the VTPR channels and has the merit of consuming only a small amount of computer time in practical use.

4. Results of comparisons of retrieved and actual $B(T_c)$ and $B(T_s)$ for the dependent sample

The R_i calculated from the model atmospheres using equation 1 and the functions expressing the τ_i and F_i in terms of $B(T_c)$ and $B(T_s)$ have been used to retrieve values of the $B(T_c)$ and $B(T_s)$ for comparison with actual values calculated directly from the model atmospheres ^{and surfaces.} For this purpose the following algorithm was used, incorporating an iterative determination of $B(T_c)$ and $B(T_s)$:-



It was found in practice that the difference between successive approximations to $B(T_6)$ and $B(T_7)$ usually fell to less than 0.04 RU in 5 or 6 iterations, from any reasonable first guess.

(i) Test of effectiveness of equations 4 to 8

Equations 4 to 8 were developed in order to retrieve separately the $B(T_c)$ and $B(T_s) \leftarrow$ from the R_i . To demonstrate their effectiveness, the R_i for the January mean atmospheres were calculated with surface temperatures up to 8°K different from the nominal value. These were then used to retrieve the $B(T_c)$ and $B(T_s) \leftarrow$. In table 5 we give the average change in the retrieved $B(T_c)$ and $B(T_s) \leftarrow$ for a unit change in the assumed $B(T_s) \leftarrow$. The retrieved $B(T_s) \leftarrow$ were calculated from the average values of $B(T_8)$ from channels 6 and 7 (see equations 5 and 6).

Table 5 Relative change in retrieved $B(T_c)$ and $B(T_s)\epsilon$
due to change in assumed $B(T_s)\epsilon$

| | 15°N | 30°N | 45°N | 60°N |
|------------------|--------|--------|--------|--------|
| $B(T_4)$ | +0.001 | -0.001 | 0.000 | +0.002 |
| $B(T_5)$ | +0.011 | -0.015 | -0.004 | +0.016 |
| $B(T_6)$ | +0.026 | +0.112 | -0.006 | +0.044 |
| $B(T_7)$ | -0.004 | -0.083 | -0.017 | +0.032 |
| $B(T_8)$ | +0.017 | -0.084 | -0.015 | +0.047 |
| $B(T_s)\epsilon$ | +0.868 | +0.963 | +1.017 | +1.018 |

Because of the decreasing surface contribution to the total radiation with increasing weighting function height we expect the relative change in the retrieved $B(T_c)$ to decrease with channel number. This tendency is confirmed in Table 5. Channels 6, 7 and 8 at latitude 30°N show anomalously high values; it is believed that the adopted January 30°N humidity profiles may differ in general shape from the other profiles for the month.

Apart from these anomalous values the relative changes in the retrieved $B(T_c)$ are in the range -0.02 to +0.05 while the changes in $B(T_s)\epsilon$ are in the range +0.87 to +1.02; the closeness of these ratios to zero and unity respectively confirm that equations 4 to 8 do have the required properties.

Although as an example we have only varied $B(T_s)$, changing both $B(T_s)$ and ϵ would give the same result indicating that equations 4 to 8 are applicable to the R_1 observed over any surface.

(ii) Errors of the retrieval of the $B(T_c)$ and $B(T_s)\epsilon$

In table 6 we give statistics of the difference between the retrieved and actual values of $B(T_c)$ and $B(T_s)\epsilon$ for the sample of monthly mean profiles.

Results for the 48 temperature profiles with mean moisture are quoted separately from those for the same temperature profiles in the saturated conditions; results for dry profiles have been omitted because $B(T_c)$ and $B(T_7)$ are undefined in these circumstances.

Mean values of the $B(T_c)$ and $B(T_5) \in$ for January and July, 15°N and 60°N are also given for comparison. The results can be interpreted in terms of temperature with the aid of the Black-body function in table 1.

Table 6 (Retrieved-actual) differences and monthly mean values of $B(T_c)$ and $B(T_5) \in$ for dependent sample

Monthly mean moisture atmospheres

| (retrieved-actual) differences in RU | | | | Mean values (in RU) | | | |
|---|--------|----------|--------|---------------------|--------------------|--------------------|--------------------|
| | | | | January | | July | |
| | Mean | st.error | st.dev | 15°N | 60°N | 15°N | 60°N |
| $B(T_4)$ | -0.012 | 0.015 | 0.104 | 58.8 | 50.0 | 59.4 | 60.1 |
| $B(T_5)$ | +0.072 | 0.111 | 0.694 | 80.5 | 61.4 | 81.4 | 74.5 |
| $B(T_c)$ | +0.143 | 0.236 | 1.632 | 101.4 | 73.6 | 102.0 | 87.9 |
| $B(T_7)$ | +0.242 | 0.157 | 1.090 | 115.5 | 88.3 | 111.4 | 99.4 |
| $B(T_8)$ | +0.010 | 0.261 | 1.807 | 132.1 | 101.1 | 133.2 | 113.3 |
| $B(T_5) \in$ | +0.221 | 0.100 | 0.692 | 141.0 | 114.3 | 142.8 | 118.9 |

Saturated atmospheres

| (retrieved-actual) differences in RU | | | | Mean values(in RU) | | | |
|---|--------|----------|--------|--------------------|--------------------|--------------------|--------------------|
| | | | | January | | July | |
| | Mean | st.error | st.dev | 15°N | 60°N | 15°N | 60°N |
| $B(T_4)$ | -0.005 | 0.003 | 0.018 | 57.8 | 49.8 | 58.6 | 59.8 |
| $B(T_5)$ | +0.242 | 0.057 | 0.398 | 78.5 | 61.7 | 79.2 | 74.9 |
| $B(T_6)$ | +0.166 | 0.123 | 0.855 | 95.4 | 74.3 | 96.0 | 88.0 |
| $B(T_7)$ | +0.057 | 0.071 | 0.495 | 95.3 | 85.1 | 95.2 | 92.0 |
| $B(T_8)$ | +0.062 | 0.221 | 1.534 | 121.4 | 98.6 | 123.5 | 110.1 |
| $B(T_5) \in$ | +1.104 | 0.241 | 1.674 | 141.0 | 114.3 | 142.8 | 118.9 |

From the values in table 6 it can be seen that the $B(T_c)$ are retrieved with a smaller error and the $B(T_s)\epsilon$ with a larger error in saturated than in average moisture conditions as indicated by the standard deviations of the differences. This is to be expected because as the moisture content increases the τ_c decrease, reducing the surface and increasing the atmospheric contributions to the radiance.

The standard deviation of the differences decreases rapidly with the height of the weighting function except for channel 7 which appears to be retrieved with a greater accuracy than expected. Several of the mean differences, although small, depart significantly from zero (judging from their standard errors). No attempt has been made here to reduce these differences or their standard deviations by "tuning" the various functions shown in figures 3 and 4, or the constants in tables 3 and 4.

An examination of the individual differences (not shown) for the atmospheres with the mean moisture profiles confirmed that those for channels 6, 7 and 8 at latitude 30° are anomalously large compared with other latitudes for the period October to March. This effect is not apparent for the saturated moisture profiles which indicates that it is not the temperature profiles which are anomalous at this latitude but the monthly mean moisture profiles.

Even in the most unfavourable conditions the standard deviations of the (retrieved-actual) differences in $B(T_c)$ and $B(T_s)\epsilon$ are always less than 12% of the difference in their mean values at 15°N and 60°N . This indicates that values of $B(T_c)$ and $B(T_s)\epsilon$ retrieved in the way described in section 3 should be capable of resolving at least the largest global patterns of atmospheric and surface radiation.

5. Sources of VTPR clear radiances

i) Clear radiances deduced from the variation of cloudy radiances over limited areas.

The National Environmental Satellite Service (NESS) of the U.S. have developed a technique for deducing the clear radiance in channels 1 to 7 of the VTPR given the clear radiance in the window channel 8 (reference 2). Briefly it depends on the assumption that the cloudy radiance in channel 8 and any other channel i for two closely situated VTPR fields of view containing differing cloud amounts are related by the linear equation $R_i = A_i R_8 + B_i$. A knowledge of the clear R_8 which is calculated from T_s and ϵ leads immediately to an estimate of the clear radiances in the other seven channels. The A_i in the above equation vary with the height of the cloud-top and so, in practice, several estimates of the R_i for areas up to 500 km square are combined to reduce the scatter due to variations in the cloud top height and also due to instrumental noise. Clear radiances can only be produced by this method over the sea; over land T_s and ϵ are not usually well known.

Clear radiances of this type are potentially available from NESS which produces them globally as an integral part of the SIRS operational sounding programme. They are also produced in Met O 19 from VTPR direct read-out data for the north-eastern Atlantic area. These clear radiances can be processed as described in this paper with due regard to the following points.

- a. Errors in R_8 lead to errors in R_i through their relationship $R_i = A_i R_8 + B_i$. The expression for $B(\tau_c)$ has no power to suppress these errors but their effect may be small if the cloud-top height happens to result in a value of A_i nearly equal to τ_i/τ_8 .
- b. Since R_8 is not an observed value there is little point in using it to deduce T_s which is used to calculate it initially.

2) Directly observed clear radiances

It is possible that directly observed VTPR clear radiances can be obtained within known cloud-free areas. Such areas could be detected by reference to the visual and infra-red cloud-pictures produced by the Scanning Radiometer which accompanies the VTPR on the NOAA Spacecraft. The two instruments, which are entirely independent, observe the same area simultaneously but there may be difficulties in registering the two types of observations. The field of view of the VTPR near the nadir is about 60 km square and adjacent observations are contiguous so that in principle a cloud-free area of 120 km square would be expected to contain at least one cloud-free VTPR observation. Areas of this size are likely to be removed from regions of meteorological interest (near fronts and in depressions), which may reduce their usefulness. However such observations would be ideal because all the radiances would be observed and independent (including R_g) and this would result in independent estimates of the $B(T_c)$ and $B(T_s)\epsilon$ over both land and sea. Over areas of known ϵ , such as the sea, T_s could then be calculated.

Over extensive clear areas, $B(T_c)$ and $B(T_s)\epsilon$ could be retrieved for each contiguous VTPR observation. Such fields of observations made over coastlines separating cool seas and warm land (or vice-versa) would indicate whether or not the methods described are effective in retrieving surface and atmospheric components by the absence or presence of similar discontinuities in the fields of $B(T_c)$ and $B(T_s)\epsilon$. Observations overland would also increase the chances of making comparisons of meteorological parameters deduced from the T_c , such as thicknesses and water vapour contents, and those measured by radio-sondes.

REFERENCES

1. FRITZ S et al "Temperature Sounding from Satellites NOAA Tech. Report
NESS 59, July 1972.
2. McMILLIN L et al "Satellite Infrared Soundings from NOAA Spacecraft".
NOAA Tech Report NESS 65, September 1973.

November 1976

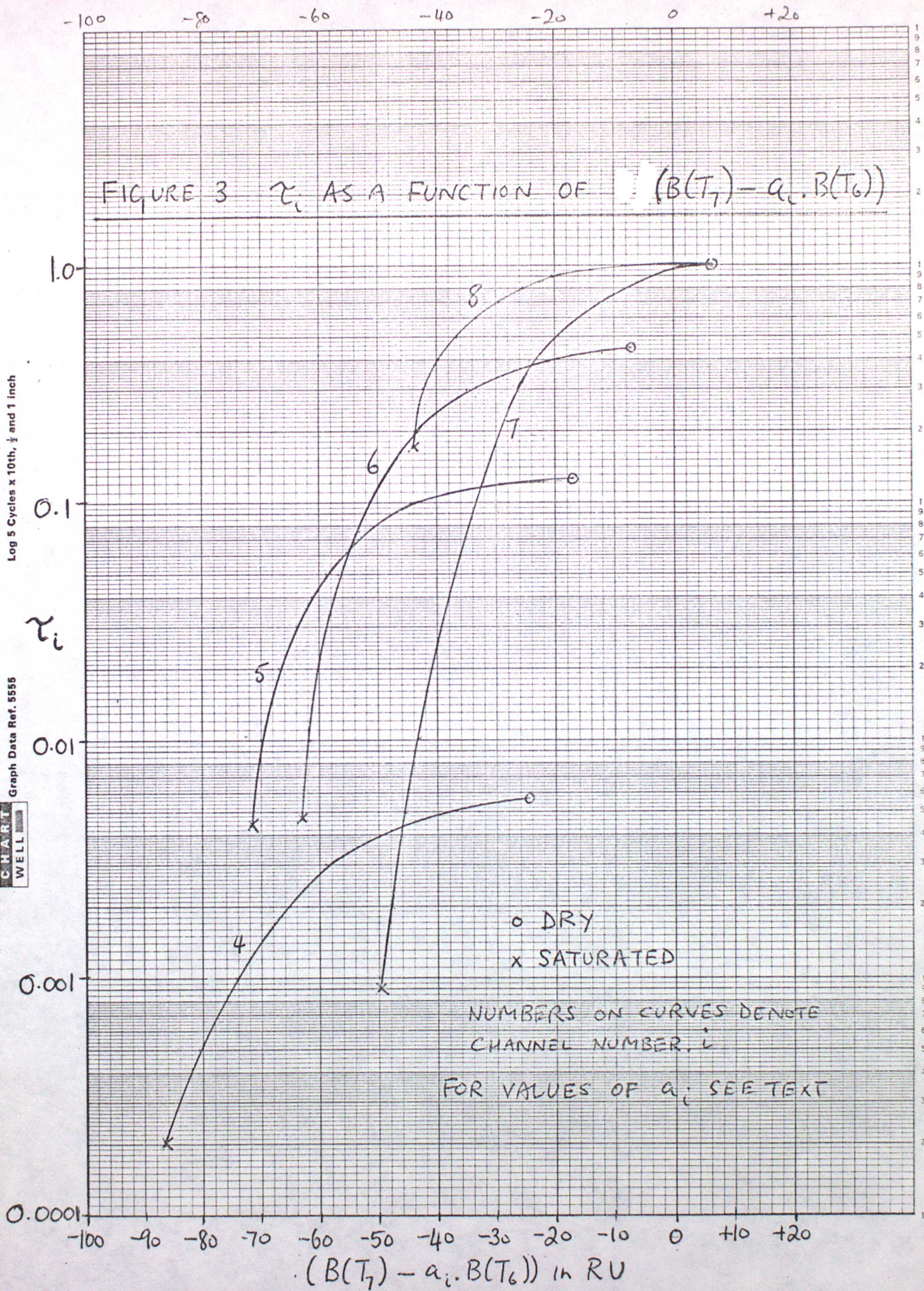


FIGURE 1 τ_0^D FOR LOW-LATITUDE TEMPERATURE PROFILE

IN DRY AND SATURATED CONDITIONS

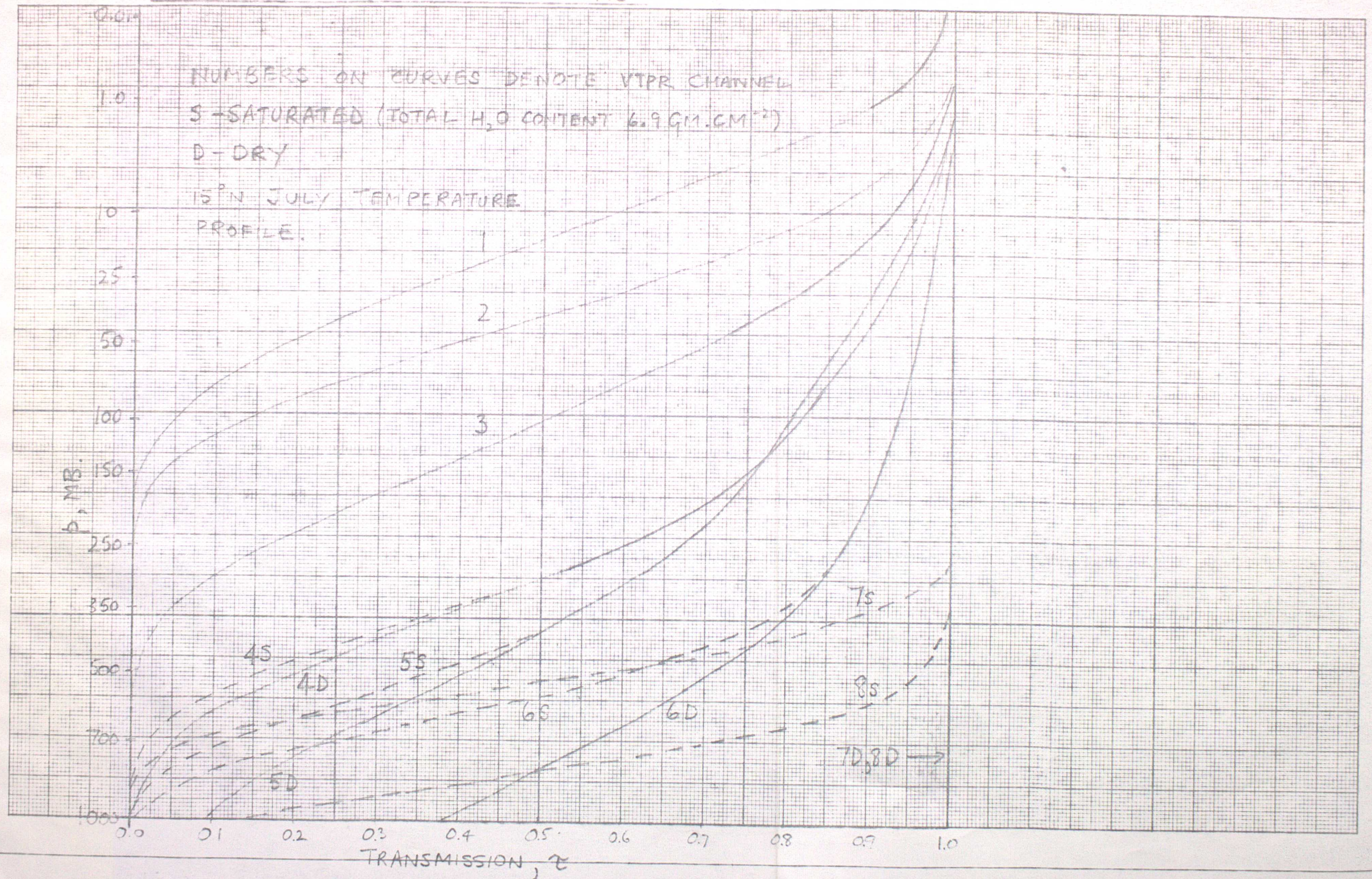


FIGURE 2 WEIGHTING FUNCTIONS FOR LOW-LATITUDE TEMPERATURE

PROFILE IN DRY AND SATURATED CONDITIONS.

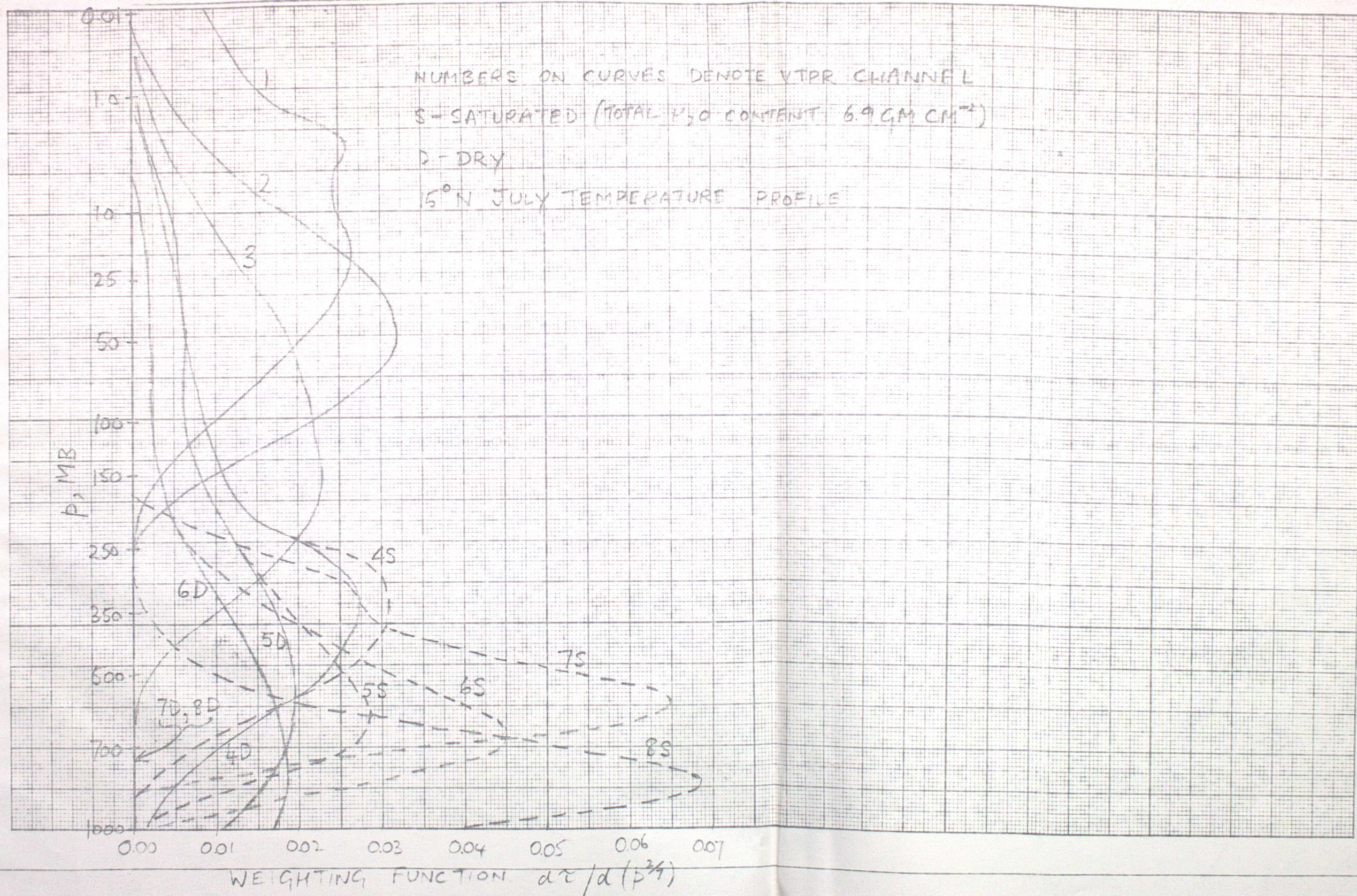


FIGURE 4. F_i AS A FUNCTION OF $(B(T_7) - b_i \cdot B(T_6))$

